NEW APPROACH TO UNDERSTAND MARINE BOUNDARY LAYER CHARACTERISTICS DURING DIFFERENT MONSOON REGIMES OVER PALAU IN PACIFIC OCEAN

U. V. Murali Krishna[1], K. Krishna Reddy[1], S. Venkata Raju[2] & Ryuichi Shirooka[3]
[1]Department of Physics, Yogi Vemana University, Kadapa-516003, Andhra Pradesh, India
[2]Dantuluri Narayana Raju College, Bhimavaram – 534202, Andhra Pradesh, India
[3]Research Institute for Global Change, Japan Agency for Marine-Earth Science and Technology (JAMSTEC), Yokosuka, Japan

ABSTRACT

A new algorithm is proposed to determine the marine boundary layer (MBL) height using a wind profiler radar and a ceilometer. For this, four year observational data from wind profiler radar and laser ceilometer installed at Palau islands in Tropical Western Pacific Ocean is utilized. We observed the diurnal and seasonal variation in the marine boundary layer height using this new algorithm. The results show a fairly good agreement with the normal peak detection method. We utilized 'new algorithm' for understanding of MBL variations during westerly/easterly monsoon periods. It is noticed that multiple forcing mechanisms are primarily responsible for the shallow marine boundary-layer heights observed during westerly monsoon period.

KEYWORDS: *Marine boundary layer, Monsoon, wind profiler radar, ceilometers, Bayesian Selection Method*

I. INTRODUCTION

The Atmospheric boundary layer (ABL) is the lowest layer (1–3 km) of the atmosphere and is characterized by turbulent fluctuations that induce mixing [1, 2]. ABL over land and ocean surface is quite different because of the differing dynamic and thermodynamic characteristics of both the surfaces. The structure and characteristics of the ABL over the oceanic surface, often known as the Marine Boundary Layer (MBL) plays an important role in regulating the surface energy and moisture fluxes and in controlling the convective transfer of energy and moisture to the free atmosphere [3]. However, the open ocean measurements of MBL structure are generally difficult due to unavailability of a stable platform over the oceanic surface. A few field experiments like the Atlantic Trade wind Experiment (ATEX) [4], Global atmospheric research program Atlantic Tropical Experiment (GATE) [5], Tropical Ocean Global Atmosphere (TOGA), TOGA and Coupled Ocean Atmosphere Response Experiment (TOGA-COARE) [6] etc. carried out to study the structure and characteristics of the Marine Atmospheric Boundary Layer over the equatorial pacific regions and the Atlantic Ocean [7, 8] during the last three decades.

Due to lack of direct measurements of boundary layer height and of suitable measurements that could be used to estimate it [9], the boundary layer height is less common in the climatological literature. This problem may be partially remedied through analysis of new data sources like observations by radio occultation measurements from global navigational satellite systems [10, 11], aerosol observations from satellites [12], Lidar [13] and Sodar [14]. Other types of observations, including Wind-profiling and boundary layer Radar [15, 16] and Ceilometer [17] have been used to estimate boundary layer height.

Wind profilers are sensitive Doppler radars, designed to respond to refractive index fluctuations in clear air. Reflectivity (range-corrected signal-to-noise ratio) is a well-established product of wind profilers used to measure the boundary layer height [18]. One potential method to routinely monitor the ABL height uses the maximum value of the refractive index structure parameter C_n^2 [15]. The automatic fuzzy logic–based technique by Bianco and Wilczak [16] uses measurements of C_n^2as well as the variance of vertical velocity, which is large within the ABL, but small above it. However, the Doppler spectral width of the radar signal gives the additional information on boundary layer structure [19], which is related to the turbulence intensity. Heo et al. [20] identified the ABL height by including the vertical profiles of Doppler spectral width of wind-profiling radar data. All these measurements concerned with planetary boundary layer studies only. So far there were no extensive studies on MBL variation over the globe. Hence for the first time an algorithm is developed to estimate the vertical structure of the MBL. With this new algorithm approach we observed the diurnal and seasonal variations in MBL height over the Western Tropical Pacific Ocean.

II. LOCATION AND DATA

The Republic of Palau is an archipelago of about 350 m high and low islands located in the most western part of the Caroline Islands of the Southwestern Pacific. Situated at latitude 7º 20’ N and longitude134º 28’ E (Fig.1), the Palau islands are almost 800 kilometers equidistant west of the Philppines, north of Irian Jaya and southeast of Guam. Aimeliik is located in the southwest corner of Babeldaob [in the Palau (508 Sq. km) archipelago], which is one of the largest islands in the western Pacific Ocean. Babeldaob Island is partly elevated limestone and partly volcanic. The vegetation in this island varies from the mangrove swamps of the coast, with trees often from 10–16 meters high; to the savannah type grasslands of the near interior which support palms and pandanus, and the densely forested valleys further inland.

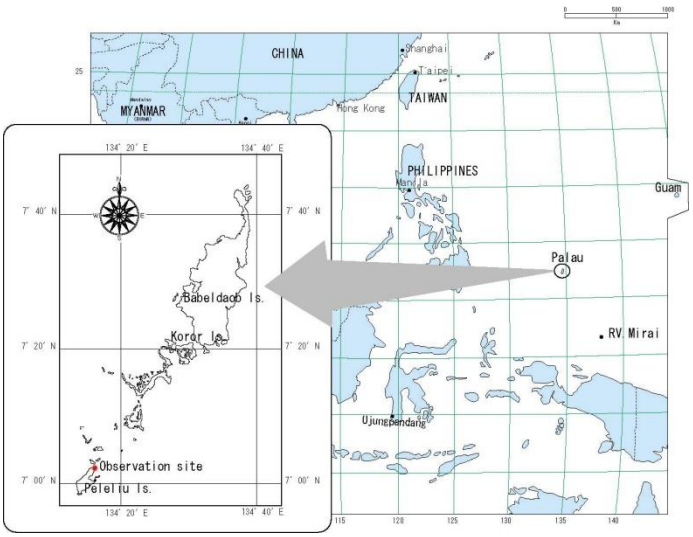

Fig.1: Map of the western Pacific region. Inset Enlarged map of Islands of Palau

Japan Agency for Marine-Earth Science and Technology (JAMSTEC) is carrying out research at Palau Islands focusing on the Pacific Area Long-term Atmospheric observation for Understanding of climate change (PALAU) project to understand the mechanism of cloud-precipitation processes and air-sea interactions over the warm water pool, focusing on seasonal and intra-seasonal variations. We have analyzed four year (April 2003 to March 2007) variations of the marine boundary layer heights on monthly basis over Palau region. The wind profiler radar (WPR) is used to estimate the boundary layer height by examining the vertical structure of reflectivity. When the wind profiler is running, an estimate is produced approximately every 4-6 minutes with a vertical resolution of 200 meters. False estimates can occur when non-precipitation artifacts produce the same patterns as precipitation. Observations with the WPR were carried out fairly continuously from 01 April, 2003 to 31 March, 2007. A total of 1140 days of wind profiler data are available until March 2007 for analysis. During the observational period, there are several days data is not available. In addition to the WPR data, we

utilized back scatter coefficient of the ceilometer, upper air data from the Koror Radiosonde obtained from the website http://weather.uwyo.edu/upperair/sounding.html and surface solar radiation from Automatic Weather Station for the above period (01 April 2003 to 31 March 2007).

III. ALGORITHM FOR MBL HEIGHT DETECTION

The conventional methods [15] used for the estimation of MBL height during heavy rainfall cases and severe convection prone for errors. Hence, we developed a new method which applies a time-dependent criterion of selection between the various stratifications as detected by a standard gradient approach (Fig. 2). The method is statistically based and is designed to select the most likelihood MBL height between all the detected stratifications. Firstly, the ceilometer estimate of MBL heights is retrieved by the standard gradient method is compared with the radiosonde virtual temperature or mixing ratio profiles. This is accomplished by merging information of MBL height from WPR with the diurnal evolution of MBL as predicted by the ceilometer. The two MBL heights (WPR and ceilometers) are combined in an optimal way using Bayesian data assimilation technique [21] to select the actual evolution of MBL height.

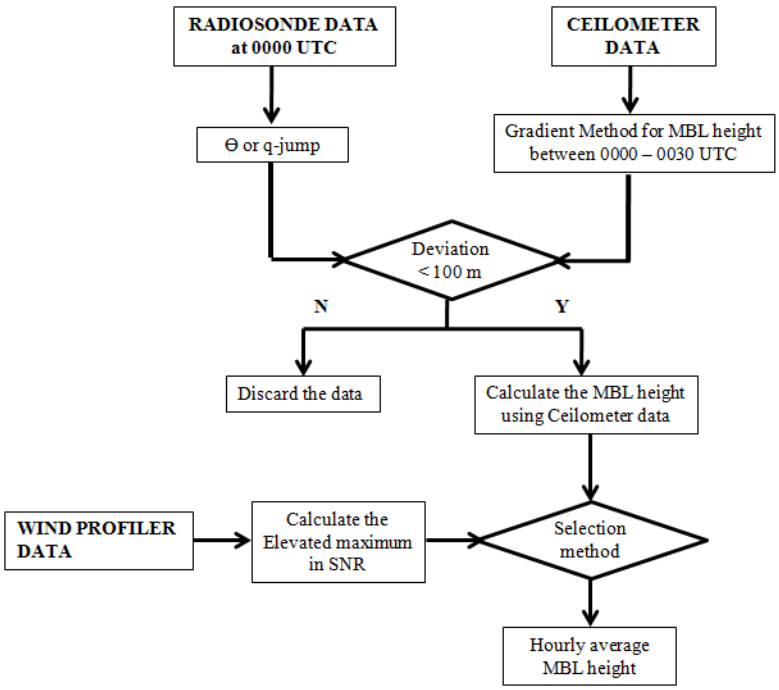

Fig. 2: Algorithm for the detection of MBL height using Radiosonde, ceilometers and WPR.

In the Bayesian selection method the time information is exploited by employing a physical model of the boundary layer evolution. The so-called bulk or slab model, [22-24] is used to estimate the boundary layer height. Effectively the Bayesian selection method is independent of the choice of the underlying boundary layer model and other. A climatological solution of the model provides the background (or "first guess") hypothesis of a possible boundary layer evolution for the day. Then an analysed model trajectory is found that minimises, in statistical sense, the distance between the background prediction and the actual boundary layer heights. The analysis vector, is a smooth solution of the physical model, and contains height estimations. If hc indicates the vector with the m daily boundary layer height estimates as derived applying a threshold to the gradient analysis of the ceilometers data and hw is the equivalent vector containing the model estimations, then an optimal combination of these information which is the analysed solution of the model i.e. boundary layer height. We compared the MBL height detected by this new algorithm with the normal peak detection algorithm (Fig. 3). A good agreement exists between the two MBL detections. The peak detection algorithm follows the actual variability of MBL height in the morning hours where as it deviates in the afternoon hours. Also it shows higher values throughout the day.

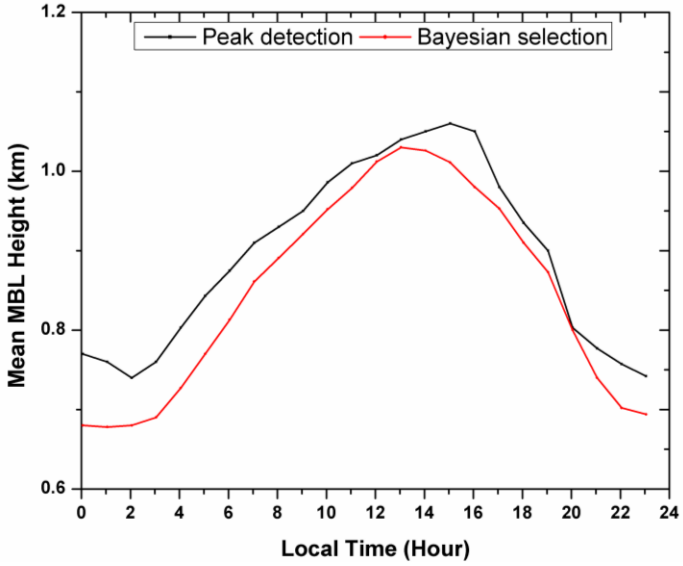

Fig. 3: Comparison of MBL heights detected using Bayesian selection method with normal peak detection algorithm

IV. RESULTS

4.1. Evolution of Marine Boundary Layer

Wind profiler offers the unique ability to directly measure vertical motion profiles through precipitating and non-precipitating cloud systems [25]. So wind profiler radars can be used to determine the MBL height during both precipitating and non-precipitating events. As an example, the smoothed hourly averaged MBL height over Palau on 10th July 2004 (non-precipitating event) is shown in Fig. 4. The MBL height is not at its minimum in the midnight. This is because previous days MBL known as residual layer present until 0400 LT. When the amount of incoming solar radiation increases in the morning hours, then MBL height also increases until afternoon. When the solar elevation decreases, the available energy is small, so the thermally-driven turbulence decays and vertical mixing decreases and the MBL height also decreases. The MBL height is at its maximum at about 1300 or 1400 LT.

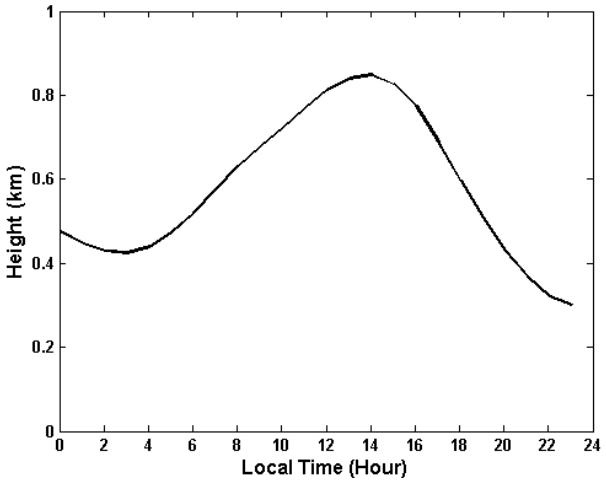

Fig. 4: Smoothed hourly average of MBL height during 10th July, 2004.

Time series of the daily maximum MBL height, as a function of Julian day of the year, are presented in Fig. 5, showing both individual daily values and a smoothed 5-day running mean. The smoothed MBL height is at or near its maximum in the month of April, before the onset of westerly monsoon period and then decreases with time until July, increases slightly and then decreases again reaching its

minimum values during the month of September. The MBL height partially recovers to a second but lower set of peaks at the end of westerly monsoon period, then increases again.

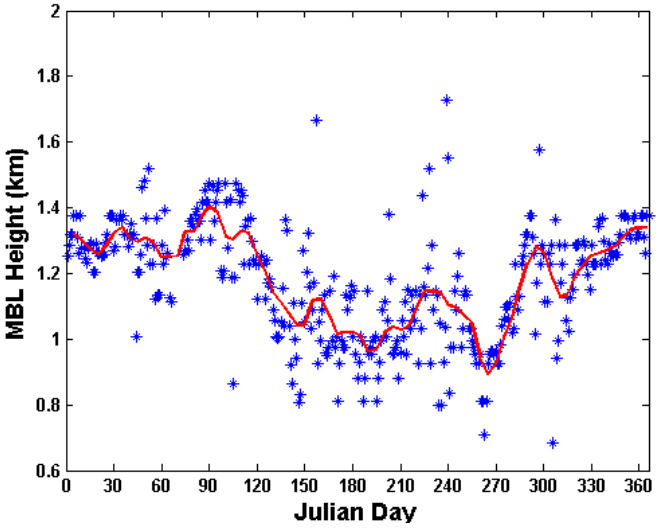

Fig. 5: Time series of maximum daily boundary-layer depths (km) as a function of the Julian day of the year (*blue stars*). The *red line* is the smoothed interpolation of the data.

4.2. Annual Variability of Marine Boundary Layer

Fig. 6 shows the monthly averaged diurnal variation of MBL height during 2003 to 2007. The months of February March and April show the longest and highest MBL heights during which the average sunshine hours are more and the months August and September the lowest MBL height, corresponding to the lowest average sunshine hours.

The study period is classified into westerly and easterly monsoon regimes [26] (Table 1). The onset of westerly monsoon occurred between June and July and the withdrawal occurred between September and December (Easterly monsoon). The present observations are categorized as non-precipitating, easterly and westerly monsoon convective days. Here convective day implies that the precipitation has taken place during that day, which is subjective. Figure 7(a) shows the evolution of MBL on two non-precipitating days (29th April and 26th September 2004). During non-precipitating days MBL is forming at morning 0600 hrs and afterwards, the MBL grows steadily and reaching its peak at about 1200-1300 hrs and coming down thereafter. The interesting feature observed on these days is that the MBL height deceases to the lower heights gradually after 1200-1300 hrs. This happens when buoyancy flux at the marine surface decreases slowly which in turn results in poor surface forcing and the shallow MBL.

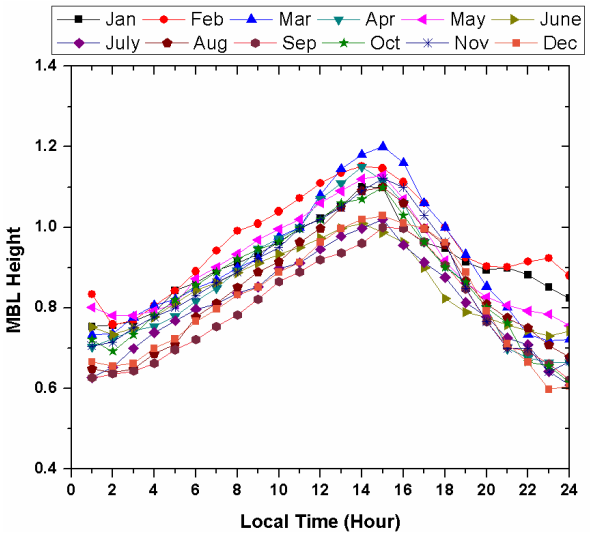

Fig. 6: Monthly-averaged diurnal MBL cycle for the period April, 2003 to March, 2007.

Table.1: Classification of Easterly and Westerly monsoon period in 2003, 2004, 2005 and 2006.

Year	Easterly Regime	Easterly Regime
2003	Mar, Apr, Dec	May, Jun, Jul, Aug, Sep, Oct, Nov
2004	Jan, Feb, Mar, Apr, May, Dec	Jun, Jul, Aug, Sep, Oct, Nov
2005	Jan, Feb, Mar, Apr, May	Jun, Jul, Aug, Sep, Oct
2006	Jan, Feb, Mar, Apr, Nov	Jun, Jul, Aug, Sep, Oct

Figure 7(b) shows the evolution of MBL on two days i.e., (16th March and 09th May 2004) during easterly monsoon period. On these days, the MBL shows more or less similar features like the non-precipitating days during morning hours. The striking feature in the present case is that the MBL is continuously growing after 1200 hrs also. The MBL heights are also very high with an increasing trend up to 1500 hrs, after which the precipitation is observed until 2000 hrs. The deepening of the MBL is observed in the late afternoon in the present case, whereas it is observed exactly at the midday on the non-convective days. Figure 7 (c) shows the evolution of MBL on two days i.e., (31st July and 18th August 2004) westerly monsoon period. On these days, a different scenario has been observed. A shallow MBL confined to about 1.1 km is observed on both the days. This is because during the westerly monsoon, boundary layer will be rich in moisture. So, most of the radiation will be utilized for the evaporation process, which results in a shallow MBL. One more cause for the shallow MBLs during the westerly monsoon days may be due to the increased upper level clouds that can reduce the incoming solar radiation. Similar features have been observed on most of the days in each category during the observational period.

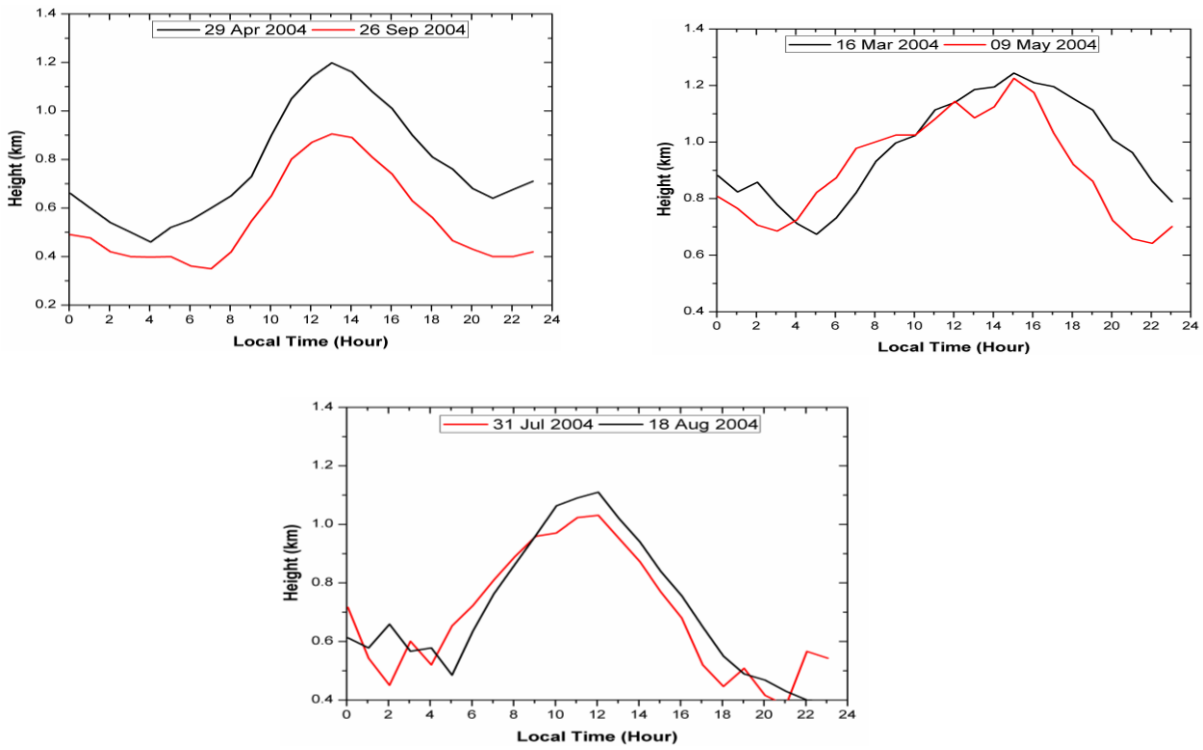

Fig. 7: Evolution of MBL on two (a) Non-precipitating (b)Easterly monsoon precipitation (c) Westerly monsoon precipitation days.

To explain the shallow MBL heights during the westerly monsoon period, we investigated the effect of surface solar radiation and low level cold air advection on MBL height. Surface solar radiation plays an important role in driving the MBL, and variations due to clouds or aerosols can have a pronounced effect on MBL height. Table 2 contains monthly means of solar radiation (W m^{-2}) and the daily maxima solar radiation (W m^{-2}). Overall, the large values of both solar radiation measures for the easterly monsoon period are indicative of mostly cloud-free conditions. The daily maximum MBL heights occur in April with values of approximately between 1.2 to 1.5 km, (Fig. 5), decreasing

to 0.9 to 1.1 km in September. Due to large solar radiation during April, maximum MBL heights are observed.

Table.2: Monthly mean solar radiation (top number); and monthly mean hourly maximum solar radiation, *SR* (bottom number).

Month	Jan	Feb	Mar	Apr	May	Jun	Jul	Aug	Sep	Oct	Nov	Dec
Mean SR	194.9	206.3	212.3	232.2	178	198.3	186.9	213.4	214	210.1	198.9	189.5
Max SR	832.9	814.7	804.3	860.2	684.6	745.7	743	797.2	814.1	845.4	796.6	710.5

Cold-air advection within the boundary layer can help reduce MBL heights by counter-acting the warming due to surface heating from solar radiation. Figure 8 shows temperature advection for both the easterly and westerly monsoon periods. The advection is calculated as the temperature difference between monsoon period and the average temperature for the whole observational period, multiplied by the westerly wind component. Increased cold-air advection during the westerly monsoon period is evident, especially at lower levels and afternoon to evening hours. The strongest cold-air advection for these months begins in the early afternoon hours, after which the MBL decreases its height gradually. This cold-air advection is associated with the push of marine air into the inland region that occurs with the afternoon sea-breeze circulation. Low-level cold-air advection will increase the stratification and will counteract the warming due to solar insolation, and will contribute to the shallower MBL heights during westerly monsoon period.

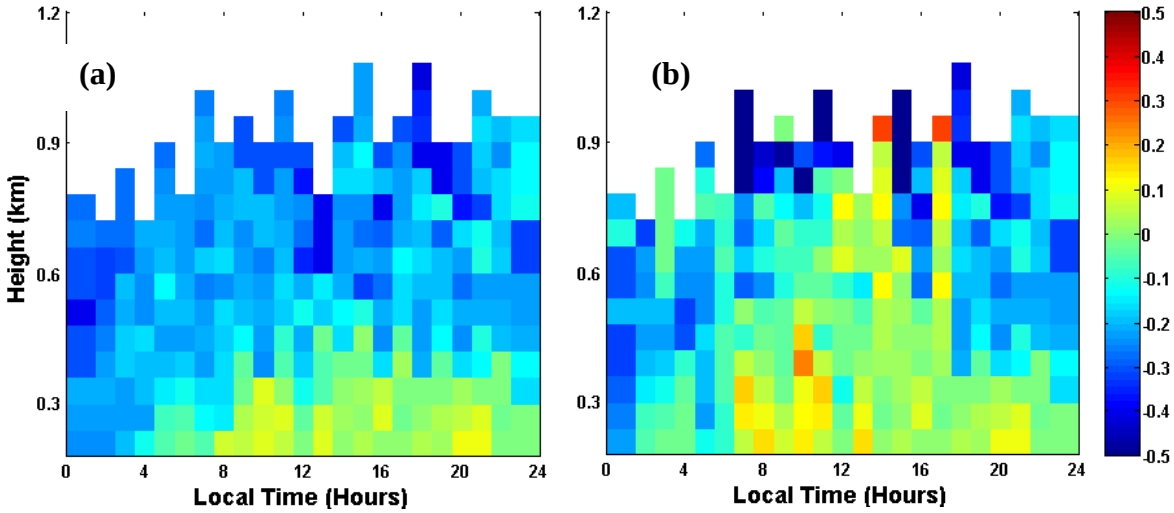

Fig. 8: Diurnal mean time–height cross section of virtual temperature advection for (a) Easterly (b) Westerly monsoon period.

V. CONCLUSIONS

A new algorithm for MBL height determination has been developed and evaluated its performances using Radiosonde, ceilometers and WPR observations over Palau islands in the Tropical Western Pacific Ocean. Observational results obtained from our algorithm show a good agreement with MBL estimated by normal peak picking method. Using new MBL height detection algorithm, the diurnal evolution and its seasonal variability has been investigated. The MBL height shows a diurnal variation with its maximum in the afternoon and decreases slowly reaching its minimum in the night. The seasonal variability of MBL height shows a maximum in the month of April and minimum in the month of September. The effect of surface solar radiation and low level cold air advection on MBL height is investigated. It is clear that, surface solar radiation is responsible for the maximum MBL height in the easterly monsoon period and cold air advection from the surrounding marine atmosphere is responsible for the shallow MBL heights during the westerly monsoon period.

VI. FUTURE WORK

This study deals with the diurnal and seasonal variation in the marine boundary layer height during Easterly and Westerly monsoon periods over Palau, Pacific Ocean. We are planning to extend our study to Gan Islands in the southern hemisphere to understand diurnal and seasonal variability of convective activity in both the hemispheres.

ACKNOWLEDGEMENTS

Original data was collected and is provided by Institute of Observational Research for Global Change (IORGC), Japan Agency for Marine-Earth Science and Technology (JAMSTEC). We also acknowledge to University of Wyoming for providing the upper air radiosonde data at their website at http://weather.uwyo.edu/upperair/sounding.html.

REFERENCES

[1]. White, J. M., Bowers, J.F., Hanna, S.R., Lundquist, J.K., (2009) Importance of using observations of mixing depths in order to avoid large prediction errors by a transport and dispersion model. J Atmos Ocean Technol **26,** 22–32.

[2]. Seibert P., F. Beyrich, S. E. Gryning, S. Joffre, A. Rasmussen, and P. Tercier, (2000) Review and inter comparison of operational methods for the determination of the mixing height. Atmos. Environ., **34**, 1001–1027.

[3]. Kloesel, K. A. and Albrecht, B. A., (1989) Low-level Inversions over the Tropical Pacific thermodynamic Structure of the Boundary Layer and the above Inversion Moisture Structure. Monthly Weather Review. **117**, 87-101.

[4]. Dunckel, M., Hasse, L., Krugermeyer, L., Schriever, D. and Wucknitz, J. (1974) Turbulent fluxes of momentum, heat and moisture in the atmospheric surface layer in the sea during ATEX: Atlantic Trade Wind Experiment. Boundary Layer Meteorol. **6,** 81–106.

[5]. Hasse, L., J. Wucknitz, G. Kruspe, V. N. Ivanov, A. A. Shuskov, I. V. Nekrasov, J. A. Volkov, B. M. Koprov, L. G. Elagina, J. Muller-Glewe and H. Hinzpeter. (1975) Preliminary report on determination of fluxes by direct and profile method during inter comparison II a. Global Atmospheric Research Program, GATE Rep. No 14, **2**, 267–277.

[6]. Fairall, C, W., Bradley, E, F., Rogers, D, P., Edson, J, B and Young, G, S. (1996) Bulk parameterization of air-sea fluxes for Tropical Ocean-Global Atmosphere Coupled-Ocean Atmosphere Response Experiment. J. Geophys. Res., doi: 10.1029/95JC03205, **101(C2)** 3747–3764.

[7]. Augstein, E., H. Riehl, F. Ostapoff and V. Wagner, (1973) Mass and Energy Transports in an Undisturbed Atlantic Trade Wind Flow. Monthly Weather Review. **101**, 101-111.

[8]. Firestone, J. K. and Albrecht, B. A., (1986) The Structure of the Atmospheric Boundary Layer in the Central Equatorial Pacific during January and February of FGGE. Monthly Weather Review. **114**, 2219-2231.

[9]. Liu, S., and X.-Z. Liang (2010) Observed diurnal cycle climatology of planetary boundary layer height, J. Clim., **23**, 5790–5809.

[10]. Guo, P., Y.-H. Kuo, S. V. Sokolovskiy, and D. H. Lenschow (2011) Estimating atmospheric boundary layer depth using COSMIC radio occultation data, J. Atmos. Sci., **68**, 1703–1713.

[11]. Ao, C. O., D. E. Waliser, S. K. Chan, J.-L. Li, B. Tian, F. Xie, and A. J. Mannucci, (2012) Planetary boundary layer heights from GPS radio occultation refractivity and humidity profiles, J. Geophys. Res., **117**, D16117, doi:10.1029/2012JD017598.

[12]. McGrath-Spangler, E. L., and S. Denning (2012) Estimates of North American summertime planetary boundary layer depths derived from space-borne lidar, J. Geophys. Res., doi:10.1029/2012JD017615.

[13]. Tucker, S. C., C. J. Senff, A. M. Weickmann, W. A. Brewer, R. M. Banta, S. P. Sandberg, D. C. Law, and R. M. Hardesty (2009) Doppler lidar estimation of mixing height using turbulence, shear, and aerosol profiles, J. Atmos. Oceanic Technol., **26**, 673–688.

[14]. Lokoshchenko, M. A. (2002) Long-term sodar observations in Moscow and a new approach to potential mixing determination by radiosonde data, J. Atmos. Oceanic Technol., **19**, 1151–1162.

[15]. Angevine, W. M., A. B. White, and S. K. Avery, (1994) Boundary layer depth and entrainment zone characterization with a boundary-layer profiler. Boundary Layer Meteorology, **68,** 375–385.

[16]. Bianco, L., and J. M. Wilczak, (2002) Convective boundary layer depth: improved measurement by doppler radar wind profiler using fuzzy logic methods. J. Atmos. Oceanic Tech, **19**, 1745-1758.

[17]. van der Kamp, D., and I. McKendry (2010) Diurnal and seasonal trends in convective mixed layer heights estimated from two years of continuous ceilometer observations in Vancouver BC, Boundary Layer Meteorol., **137**, 459–475.
[18]. Cohn, S. A., and W. M. Angevine, (2000) Boundary layer height and entrainment zone thickness measured by lidars and wind-profiling radars. J. Appl. Meteor., **39,** 1233–1247.
[19]. Gossard, E. E., R. R. Chadwick, T. R. Detman, and J. Gaynor, (1984) Capability of surface-based clear-air Doppler radar for monitoring meteorological structure of elevated layers. J. Climate Appl. Meteor., **23,** 474–485.
[20]. Heo, B., Jacoby-Koaly, S., Kim, K., Campistron, B., Benech, B and Jung, E, (2003) Use of the Doppler spectral width to improve the estimation of the convective boundary layer height from UHF wind profiler observations, J. Atmos. Oceanic Tech, **20**, 408-424.
[21]. Daley, R. (1993) Atmospheric data analysis. Cambridge University Press.
[22]. Betts, A., (1992) FIFE atmospheric boundary layer budget methods. J. Geophys. Res **97**, 18523–18531.
[23]. Carson, D., 1973. The development of a dry inversioncapped convectively unstable boundary layer. Quarterly Journal of the Royal Meteorological Society, **99**, 450– 467.
[24]. Tennekes, H., 1973. A model for the dynamics of the inversion above a convective boundary layer. J. Atmos. Sci., **30**, 558–567.
[25]. Reddy, K. K., T. Kozu, Y. Ohno, K. Nakamura, A. Higuchi, K. Madhu Chandra Reddy, V. K. Anandan, P. Srinivasulu, A. R. Jain, P. B. Rao, R. Ranga Rao, G. Viswanathan, and D. N. Rao., (2002) Planetary boundary layer and precipitation studies using lower atmospheric wind profiler over tropical India. Radio Science, **37**, doi: 10.1029/2000RS002538.
[26]. Kubota, H., R. Shirooka, T. Ushiyama, T. Chuda, S. Iwasaki, and K. Takeuchi, (2005) Seasonal variations of precipitation properties associated with the monsoon over Palau in the western Pacific, Journal of Hydrometeorology. **6**, 518–531.

AUTHORS

U. V. Murali Krishna received Post-Graduate degree in Physics from School of Mathematical and Physical Sciences, Sri Venkateswara University, Tirupati, Andhra Pradesh, India. He is pursuing Doctor of Philosophy in Atmospheric Science, department of Physics, Yogi Vemana University, Kadapa, Andhra Pradesh, India.

K. KRISHNA REDDY, Professor of Physics, Yogi Vemana University, Kadapa, Andhra Pradesh, India. He has more than 80 publications in different national and international journals in Radar Meteorology, Clouds Dynamics and Mesoscale Modeling, Ground based Remote sensors/Instrumentation for atmospheric physics, Convective Boundary Layer, Tropic Land-Atmosphere and Air-Sea Interactions and General Circulation. He received 6 national and 2 International awards in the field of Atmospheric Physics.

Samanthapudi Venkata Raju obtained M.Sc., obtained Meerut University, Uttar Pradesh in the year 1986 and Master of Philosophy from Andhra University in the year 2002. Doctor of Philosophy (PhD), thesis"Multi-sensor Observations on Microphysical characteristics of Clouds and Precipitation over Palau in Pacific Ocean" submitted to Acharaya Nagarjuna University, Guntur. Presently working as a senior Lecturer in Physics of D.N.R. College, Bhimavaram.